Pyrochlore chemistry from the Sokli phoscorite-carbonatite complex, Finland: Implications for the genesis of phoscorite and carbonatite association

MI JUNG LEE,[1]* JONG IK LEE,[2] DANIEL GARCIA,[3] JAQUES MOUTTE,[3] C. TERRY WILLIAMS,[4] FRANCES WALL[4] and YEADONG KIM[2]

[1]Geology & Geoinformation Division, Korea Institute of Geoscience & Mineral Resources, Gajeong-dong 30, Yuseong-Gu, Daejeon, 305-350 Korea
[2]Korea Polar Research Institute, KORDI, 1270, Sa-2-dong, Sangrokgu, Ansan 426-744, Korea
[3]GENERIC, Centre SPIN, Ecole des Mines de Saint Etienne, 158 Cours Fauriel, 42023 Saint-Etienne, France
[4]Department of Mineralogy, The Natural History Museum, Cromwell Road, London SW7 5BD, U.K.

The phoscorite-carbonatite complex in the Sokli alkaline-carbonatite massif, northern Finland, comprises five stages of intrusions of phoscorites and carbonatites (P1-C1, P2-C2 and P3-C3 for phoscorites and calcite carbonatites; D4 and D5 for dolomite carbonatites). The phoscorites and calcite carbonatites at Sokli usually occur as pairs with the same mineral assemblages. Pyrochlore is found in the majority of rock types in the Sokli phoscorite-carbonatite complex, shows wide compositional variation and seems to preserve evolution trends of host rocks. Crystallization of pyrochlore begins from the P2-C2 phoscorite and calcite carbonatite and continues up to the latest D5 dolomite carbonatite. Pyrochlore in the early stage P2-C2 rocks has high U and Ta contents. These elements suddenly decrease from the P3-C3 rocks, on the other hand, Th and Ce contents increase. The compositions of the late generations from the D4 and D5 rocks are close to that of an ideal end-member pyrochlore with formula $(Ca,Na)_2Nb_2O_6F$. The Nb/Ta ratio and F content of pyrochlore increase from P2-C2 to the latest D5 dolomite carbonatite. The composition and evolutionary history of pyrochlore from the phoscorites are distinguished from those of the associated calcite carbonatites. Pyrochlore from the calcite carbonatites shows larger A-cation deficiencies compared to those from the paired phoscorites. Ta and Zr contents are slightly higher in pyrochlore from the calcite carbonatites, whereas Ti is generally higher in pyrochlore from the associated phoscorites. Moreover, pyrochlore from the phoscorites always shows a longer and more complex crystallization history compared to that of the same stage carbonatites. This indicates that the chemical condition was clearly different in the two systems during the crystallization of pyrochlore. Based on these results, together with the previous mineralogical and geochemical studies on the Sokli phoscorite-carbonatite complex, we propose a liquid immiscibility process as the most possible segregation mechanism of the two associated rocks. The composition of pyrochlore in the late dolomite carbonatites is distinct and always lies on the evolutional trend of the earlier varieties. This implies that the dolomite carbonatites are the final magmatic products of the Sokli phoscorite-carbonatite system.

Keywords: pyrochlore, phoscorite, carbonatite, Sokli, liquid immiscibility

INTRODUCTION

The Kola Alkaline Province (KAP) covers an area of approximately 100,000 km^2, and is one of a few regions in the world where the Paleozoic ultramafic-alkaline magmatism is well developed (Woolley, 1989; Kogarko *et al.*, 1995; Bulakh *et al.*, 2004). There are more than 20 massifs of the Paleozoic ultramafic and alkaline rocks in the KAP, and sixteen of them contain carbonatites. A characteristic feature of the Kola carbonatites in many complexes is their close relation with phoscorites, rocks consisting essentially of apatite, magnetite and forsterite or diopside (±phlogopite or tetraferriphlogopite). Phoscorites and the paired carbonatites generally show an extremely intricate association (at the meter scale) and share the same mineral assemblages which evolve from stage to stage.

Genetic relationships between alkali silicate rocks and associated carbonatites have been examined in detail through previous experimental and isotopic studies. They show that carbonatites can originate from parental carbonated silicate melts by crystal fractionation or carbonate-silicate immiscibility (e.g., Lee and Wyllie, 1998 and references therein), and can also be generated from direct partial melting of a carbonated peridotite mantle source (e.g., Sweeney, 1994; Wyllie and Lee, 1998; Lee *et al.*, 2000).

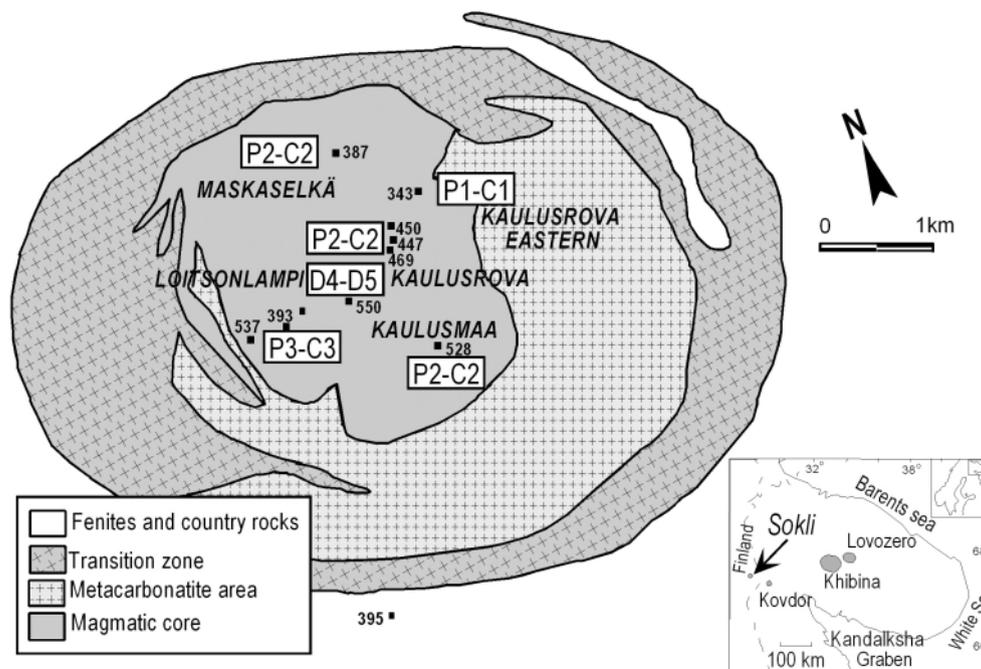*Corresponding author (e-mail: mjlee@rock25t.kigam.re.kr)

Fig. 1. Map of the Sokli alkaline-carbonatite massif (modified from Vartiainen, 1980), showing the location of sampling drill holes and distribution of five stage phoscorites and carbonatites. Inset; Map of the Kola Alkaline Province (after Bell et al., 1996).

However, there are only limited numbers of studies for phoscorite-carbonatite pairs in the KAP (Zaitsev and Bell, 1995; Dunworth and Bell, 2001; Amelin and Zaitsev, 2002; Wall and Zaitsev, 2004). These isotopic and petrographic studies suggest that phoscorites and associated carbonatites were derived from a common parental magma, however give little information on the evolution processes of the phoscorite-carbonatite magma system.

The Sokli alkaline-carbonatite massif is a member of the KAP. Compared with the other complexes, phoscorite-carbonatite rock series are well represented at Sokli. Furthermore, there are a large number of drill cores from this region, thus providing a good opportunity for carrying out a detailed study on phoscorite-carbonatite rock series.

Phoscorites and carbonatites in the Sokli alkaline-carbonatite massif show a wide compositional range and are represented by three phoscorite-calcite carbonatite groups and two varieties of dolomite carbonatites. However, characterization of their parental magmas seems to be very difficult because of the high degree of modal variability and problems of estimating the extent of volatile loss during the crystallization. Thus the mineralogical approach has been chosen to contribute to our understanding on the evolution history of the phoscorite-carbonatite system.

Pyrochlore is the main host of Nb metal in many Kola phoscorite-carbonatite complexes (PCCs). Pyrochlore

mineralization of the Sokli PCC is both quantitatively important (subeconomic) and chemically varied compared to that of the other complexes (Lee *et al.*, 2004). The Sokli pyrochlore well preserves a primary chemical zoning and incorporates a variety of HFSEs such as Ti, Nb, Ta, Th and U, depending on bulk compositions of the host rocks. Moreover, pyrochlore in the Sokli PCC is a late crystallizing mineral which is likely to bear many lines of information on the late crystallization stage, especially regarding the segregation process between the phoscorites and associated carbonatites. Therefore, a comprehensive investigation on pyrochlore from Sokli can provide important clues to understand the petrogenetic relationship between the phoscorites and conjugate carbonatites.

In this paper, we characterize the occurrences and compositional variations of pyrochlore from the Sokli PCC and document the overall evolution trends of them, and finally will discuss the segregation mechanisms of the two associated rocks.

GENERAL GEOLOGY AND PETROGRAPHY

The Sokli complex is located in the eastern Finish Lapland (67°48′ N, 29°27′ E) and intruded into Archean Belomorian group rocks at about 360 Ma (Kramm *et al.*, 1993). It was discovered in 1967 by airborne geophysical survey and its geological structure and petrology were established by extensive campaigns of drilling and
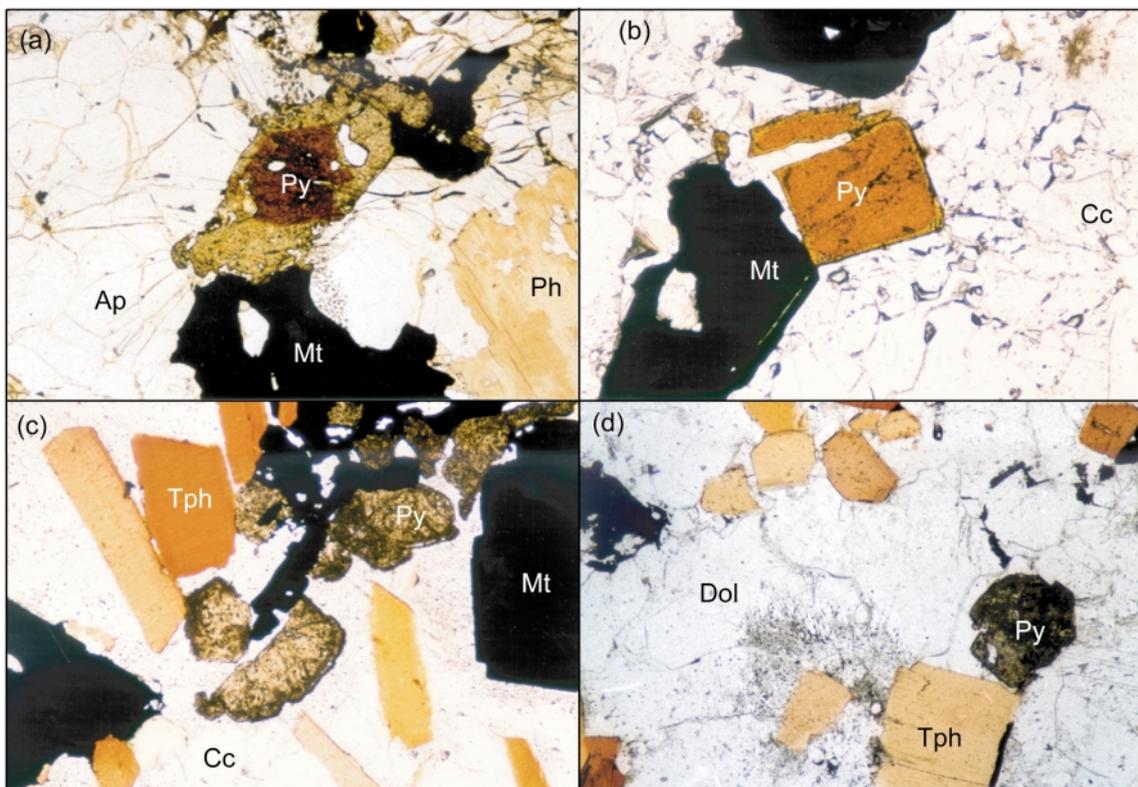
Fig. 2. Photomicroscopes of the Sokli pyrochlore; width of the photos is 2.5 mm. (a) Zoned P2 pyrochlore with U-Ta-rich dark red core and embayed Th-rich outer rim. (b) Cubic reddish brown Ta-rich pyrochlore in C2. (c) Zoned P3 pyrochlore (Th-Ce-rich yellowish cores, Th-Ce-poor resorbed outer rims). (d) Gray D5 pyrochlore with composition close to ideal end-member. Abbreviations; Py, pyrochlore; Ap, apatite; Mt, magnetite; Ph, phlogopite; Tph, tetraferriphlogopite; Cc, calcite; Dol, dolomite.

trenching with detailed geophysical investigations (Vartiainen and Paarma, 1979; Vartiainen, 1980; Lee *et al.*, 2004). The overall outline of the complex is a vertical pipe with about 6.4 km in diameter on the surface level and walls steeply dipping inward. The complex has a concentrically zoned structure that can be divided into two major zones, and is surrounded by fenite aureole of 1–2 km in width (Fig. 1).

The outer zone mainly consists of ultramafic rocks which were largely transformed into carbonate-bearing metasomatic facies by CO_2-rich fluids derived from later carbonatite injections. The relic minerals and bulk compositions indicate that the ultramafic rocks were mostly pyroxenites (Vartiainen, 1980; Lee, 2002).

The inner zone (phoscorite-carbonatite complex, PCC; also referred to as "magmatic core") is made up of multi-intrusions of phoscorites and carbonatites. Five stages of evolution have been identified on the basis of the mineral compositions and assemblages (Lee, 2002; Lee *et al.*, 2003). The first three stages comprise phoscorites and calcite carbonatites (referred to as P1 to P3 and C1 to C3, respectively), while the last two stages comprise only dolomite carbonatites (D4 and D5). The first three stages are characterized by the presence of typical silicate minerals, which are successively forsterite, phlogopite and tetraferriphlogopite from stage 1 to stage 3. Common accessory minerals also change from baddelelyite in stage 1 to pyrochlore in later two stages. This succession and diversity of the phoscorites and carbonatites are similar to those observed in the Seblyavr, Kovdor and Vuoriyarvi intrusions (Lapin, 1979; Krasnova and Kopylova, 1988; Karchevsky and Moutte, 2004). The sequence is therefore now considered as a generalized differentiation series of PCCs.

Even though a detailed structural mapping for the Sokli PCC is not available, because of poor outcrops, drill core samples show that the early stage rocks (P2-C2 and subordinate P1-C1 rocks) form the majority of the magmatic core and are intruded by the later stage rocks (P3-C3) emplaced towards the center. The late stage D4 and D5 rocks occur as dikes or veins cutting all former rocks and concentrate in a few drill cores located at the center of the complex.

The phoscorites and calcite carbonatites from the first three groups mainly consist of calcite, fluorapatite, magnetite, forsterite and phlogopite

Table 1. Average electron microprobe analyses of pyrochlores

| Sample | 387R160 | | 469R194 | | SS2 (inner zone) | | SS2 (outer zone) | | 387R73 | | 528R250 | | 343R205 | | 393R224 | |
| Rock type | C2 | | C2 | | P2 | | P2 | | P2 | | P2 | | C3 | | C3 | |
No.	6	σ	20	σ	23	σ	46	σ	13	σ	33	σ	7	σ	13	σ
Na_2O	—		0.30	0.12	5.02	0.46	5.87	0.67	5.78	0.87	5.11	0.79	5.67	2.03	0.66	0.29
MgO	0.14	0.10	—		—		—		0.11	0.17	0.06	0.07	0.10	0.21	0.04	0.03
Al_2O_3	0.08	0.03	0.03	0.02	0.02	0.02	—		0.02	0.01	0.02	0.01	0.02	0.01	0.02	0.01
SiO_2	—		—		—		0.04	0.08	0.33	0.45	0.77	0.62	—		—	
CaO	8.12	0.73	8.43	1.24	10.82	0.58	16.01	1.07	13.55	2.18	10.01	1.70	12.51	2.35	7.73	1.28
TiO_2	0.63	0.04	4.58	0.62	9.57	0.73	5.47	0.57	4.22	0.53	4.82	0.62	4.46	0.36	2.07	0.89
MnO	0.06	0.13	—		—		—		0.12	0.19	0.18	0.09	0.07	0.09	0.07	0.04
*Fe_2O_3	1.72	0.11	1.05	0.49	0.56	0.29	0.32	0.09	0.50	0.54	1.14	0.46	0.21	0.24	1.33	0.62
SrO	0.88	1.70	0.23	0.14	0.06	0.03	0.30	0.06	0.39	0.19	0.44	0.25	0.54	0.27	1.02	0.43
Y_2O_3	—		—		—		0.08	0.03	0.06	0.03	0.11	0.03	0.05	0.02	0.06	0.03
ZrO_2	2.32	0.25	2.57	0.80	1.26	0.82	1.18	0.32	0.64	0.24	2.13	1.17	0.31	0.08	4.56	1.21
Nb_2O_5	45.58	2.18	45.49	3.76	33.10	5.60	57.62	3.34	60.28	2.00	59.87	2.25	59.85	3.35	55.59	1.62
BaO	0.36	0.87	0.85	0.83	—		0.10	0.16	0.59	0.63	0.70	0.24	0.91	0.74	0.58	0.70
La_2O_3	0.09	0.06	0.07	0.03	0.05	0.02	0.18	0.03	0.16	0.03	0.27	0.06	0.41	0.18	0.18	0.03
Ce_2O_3	0.37	0.30	0.45	0.09	0.30	0.07	1.08	0.19	0.82	0.10	1.74	0.40	1.37	0.38	1.12	0.14
Pr_2O_3	0.03	0.05	—		0.04	0.04	0.06	0.06	0.03	0.05	0.03	0.05	0.03	0.05	0.05	0.04
Nd_2O_3	0.03	0.06	0.04	0.04	—		0.20	0.06	0.18	0.04	0.40	0.11	0.30	0.14	0.23	0.05
Ta_2O_5	11.53	0.48	13.91	1.65	13.80	2.16	1.91	1.97	1.87	0.25	0.31	0.12	3.98	1.42	5.21	0.48
PbO	0.77	0.10	0.54	0.12	1.05	0.19	0.09	0.03	0.03	0.03	0.04	0.05	0.03	0.05	0.29	0.07
ThO_2	2.22	0.86	1.55	0.52	0.61	0.16	4.56	1.05	4.52	0.74	5.22	0.60	2.42	0.76	3.03	0.22
UO_2	17.18	1.58	11.46	2.67	21.38	2.91	1.01	2.70	0.29	0.13	0.11	0.05	0.60	0.47	6.22	0.96
F	0.56	0.27	1.56	0.36	0.76	0.44	3.19	0.49	3.26	0.33	3.09	0.34	2.96	0.91	1.47	0.28
Sum	92.65		93.13		98.40		99.28		97.75		96.58		96.80		91.52	
-O=F	0.24		0.66		0.32		1.34		1.37		1.30		1.25		0.62	
Total	92.42		92.47		98.08		97.93		96.37		95.28		95.55		90.91	

Structural formulae calculated to 2 *B*-site cations

A site

Na	—		0.040		0.722		0.722		0.701		0.592		0.691		0.082	
Mg	0.015		—		—		—		0.011		0.005		0.010		0.004	
Ca	0.653		0.605		0.860		1.088		0.909		0.641		0.843		0.528	
Mn	0.004		—		—		—		0.006		0.009		0.004		0.004	
Sr	0.038		0.009		0.003		0.011		0.014		0.015		0.020		0.038	
Y	—		—		—		0.003		0.002		0.003		0.002		0.002	
Ba	0.010		0.022		—		0.002		0.014		0.016		0.022		0.014	
La	0.002		0.002		0.001		0.004		0.004		0.006		0.010		0.004	
Ce	0.010		0.011		0.008		0.025		0.019		0.038		0.032		0.026	
Pr	0.001		—		0.001		0.001		0.001		0.001		0.001		0.001	
Nd	0.001		0.001		—		0.004		0.004		0.009		0.007		0.005	
Pb	0.016		0.010		0.021		0.001		0.000		0.001		0.001		0.005	
Th	0.038		0.024		0.010		0.066		0.064		0.071		0.035		0.044	
U	0.287		0.171		0.353		0.014		0.004		0.001		0.008		0.088	
S cations	1.076		0.894		1.980		1.943		1.753		1.409		1.683		0.847	

B site

Al	0.007		0.002		0.002		—		0.001		0.002		0.001		0.001	
Si	—		—		—		0.002		0.021		0.046		—		—	
Ti	0.035		0.231		0.534		0.261		0.198		0.217		0.211		0.099	
Fe	0.097		0.053		0.031		0.015		0.024		0.051		0.010		0.064	
Zr	0.085		0.084		0.046		0.037		0.020		0.062		0.010		0.142	
Nb	1.547		1.378		1.110		1.652		1.706		1.618		1.702		1.604	
Ta	0.235		0.253		0.279		0.033		0.032		0.005		0.068		0.090	
S cations	2.000		2.000		2.000		2.000		2.000		2.000		2.000		2.000	
F	0.133		0.330		0.178		0.640		0.645		0.584		0.589		0.296	
% *A*-site vacancies	46.21		55.28		1.01		2.84		12.33		29.53		15.84		57.66	

(±tetraferriphlogopite). The phoscorites are usually enriched in magnetite and silicates, as well as accessory Nb-Zr minerals (baddeleyite, pyrochlore and zirconolite) compared with the paired calcite carbonatites. There are significant variations in modal compositions even within each rock type and there are large compositional gaps between calcite carbonatite and phoscorite. The compositional gaps between the phoscorite and associated calcite carbonatite is relatively small in P1-C1 (10–30 vol.% calcite in P1, 60–80 vol.% in C1); the difference increases towards P2-C2 and P3-C3, i.e., calcite carbonatites become increasingly calcite-rich, and phoscorites increasingly calcite-poor and silicates-rich. Dolomite begins to crystallize from the end of stage 3. From stage 4, carbonatite composition changes to dolomitic. The D4 dolomite carbonatite is nearly monomineralic, and is very poor in silicates, magnetite and fluorapatite. However, in the latest D5 dolomite carbonatite, dolomite is enriched in Fe and Mn, and Sr–Ba-LREE carbonates (calcian strontianite, alstonite and

Table 1. (continued)

| Sample | 393R150 | | 393R164B | | 447R172 | | 537R53 | | 450R107 | | 450R139 | | 469R179 | | 550R145 | |
| Rock type | P3 | | P3 | | P3 | | P3 | | D4 | | D4 | | D4 | | D5 | |
No.	22	σ	16	σ	14	σ	14	σ	44	σ	11	σ	14	σ	4	σ
Na$_2$O	6.83	0.94	5.05	0.61	5.54	1.26	6.34	0.89	7.48	0.23	7.38	0.45	6.78	0.67	7.80	0.33
MgO	0.03	0.05	0.05	0.04	0.07	0.03	0.06	0.11	—		—	0.02	0.04	0.10	—	
Al$_2$O$_3$	0.02	0.01	0.02	0.02	0.02	0.01	0.02	0.02	—		0.02	0.01	0.02	0.02	—	
SiO$_2$	0.76	0.69	1.66	0.25	0.57	0.39	0.09	0.29	0.25	0.15	0.62	0.50	0.40	0.32	0.08	0.01
CaO	12.81	2.49	11.64	0.52	9.89	1.30	14.75	1.97	16.40	0.54	15.85	0.68	15.08	1.44	15.51	0.24
TiO$_2$	3.37	1.39	4.26	0.32	5.50	0.48	4.98	0.64	3.93	0.99	4.00	0.24	4.15	0.27	3.57	0.56
MnO	0.03	0.04	—		0.03	0.03	0.03	0.07	—		—		—		—	
*Fe$_2$O$_3$	0.91	0.77	2.25	0.22	0.27	0.14	0.46	0.99	0.02	0.03	0.12	0.13	0.19	0.15	0.40	0.76
SrO	0.45	0.21	0.63	0.24	0.56	0.17	0.62	0.48	0.71	0.08	0.83	0.16	0.78	0.13	1.42	0.04
Y$_2$O$_3$	0.09	0.03	0.12	0.02	0.10	0.03	0.08	0.02	0.09	0.02	0.09	0.02	0.09	0.02	0.10	0.01
ZrO$_2$	0.73	0.58	1.82	0.47	0.56	0.36	0.38	0.12	0.41	0.73	0.12	0.03	0.21	0.10	0.02	0.04
Nb$_2$O$_5$	62.28	2.13	57.93	1.38	60.61	1.83	60.35	2.04	66.19	0.74	66.47	0.84	63.52	0.99	65.27	0.65
BaO	0.51	0.52	0.70	0.61	0.73	0.79	0.48	0.84	0.04	0.03	0.44	0.51	0.46	0.38	0.07	0.02
La$_2$O$_3$	0.21	0.11	0.17	0.04	0.27	0.03	0.31	0.07	0.17	0.04	0.22	0.03	0.37	0.15	0.23	0.14
Ce$_2$O$_3$	1.10	0.33	0.94	0.09	1.30	0.15	1.51	0.30	0.56	0.10	0.65	0.11	1.42	0.58	0.59	0.35
Pr$_2$O$_3$	0.04	0.06	—		0.05	0.05	0.04	0.01	0.03	0.04	0.03	0.06	0.06	0.08	—	
Nd$_2$O$_3$	0.27	0.23	0.21	0.05	0.26	0.05	0.27	0.10	0.06	0.05	0.10	0.05	0.32	0.27	0.08	0.05
Ta$_2$O$_5$	0.22	0.30	0.04	0.05	0.12	0.03	2.88	0.76	0.10	0.07	0.05	0.06	0.16	0.09	0.06	0.07
PbO	0.04	0.07	0.03	0.05	0.08	0.06	0.02	0.05	—		—		0.02	0.03	—	
ThO$_2$	4.30	1.01	3.29	0.19	6.71	0.98	1.70	0.27	0.61	0.27	0.64	0.19	1.08	0.77	0.20	0.08
UO$_2$	0.11	0.08	0.11	0.06	0.14	0.07	0.73	1.11	0.07	0.06	0.07	0.08	0.06	0.06	0.09	0.07
F	3.60	0.42	3.08	0.46	2.90	0.46	3.48	0.46	4.50	0.23	4.42	0.32	4.09	0.45	5.19	0.31
Sum	98.70		94.03		96.28		99.57		101.66		102.12		99.31		100.72	
-O=F	1.52		1.30		1.22		1.47		1.90		1.86		1.72		2.19	
Total	97.19		92.73		95.06		98.11		99.76		100.26		97.59		98.53	

Structural formulae calculated to 2B-site cations

A site

Na	0.813		0.582		0.659		0.758		0.869		0.846		0.808		0.928	
Mg	0.003		0.004		0.006		0.005		—		—		0.004		—	
Ca	0.843		0.741		0.650		0.975		1.053		1.004		0.994		1.020	
Mn	0.002		—		0.001		0.001		—		—		—		—	
Sr	0.016		0.022		0.020		0.022		0.025		0.029		0.028		0.050	
Y	0.003		0.004		0.003		0.003		0.003		0.003		0.003		0.003	
Ba	0.012		0.016		0.018		0.012		0.001		0.010		0.011		0.002	
La	0.005		0.004		0.006		0.007		0.004		0.005		0.008		0.005	
Ce	0.025		0.020		0.029		0.034		0.012		0.014		0.032		0.013	
Pr	0.001		—		0.001		0.001		0.001		0.001		0.001		—	
Nd	0.006		0.005		0.006		0.006		0.001		0.002		0.007		0.002	
Pb	0.001		0.001		0.001		0.000		—		—		—		—	
Th	0.060		0.045		0.094		0.024		0.008		0.009		0.015		0.003	
U	0.001		0.001		0.002		0.010		0.001		0.001		0.001		0.001	
S cations	1.791		1.445		1.496		1.858		1.978		1.922		1.912		2.028	

B site

Al	0.001		0.001		0.001		0.001		—		0.001		0.001		—	
Si	0.046		0.099		0.035		0.005		0.015		0.037		0.025		0.005	
Ti	0.156		0.190		0.254		0.231		0.177		0.178		0.192		0.165	
Fe	0.042		0.101		0.012		0.021		0.001		0.005		0.009		0.018	
Zr	0.022		0.053		0.017		0.011		0.012		0.003		0.006		0.001	
Nb	1.730		1.556		1.680		1.682		1.793		1.776		1.766		1.810	
Ta	0.004		0.001		0.002		0.048		0.002		0.001		0.003		0.001	
S cations	2.000		2.000		2.000		2.000		2.000		2.000		2.000		2.000	
F	0.700		0.579		0.563		0.679		0.853		0.827		0.796		1.007	
% A-site vacancies	10.46		27.76		25.20		7.09		1.11		3.90		4.40		0.00	

*No., number of spot anayses; σ, the standard deviaton; *Fe$_2$O$_3$, total iron is given as Fe$_2$O$_3$.*
C2 and C3, C2 and C3 calcite carbonatites; D4 and D5, D4 and D5 dolomite carbonatites.
P2 and P3 , P2 and P3 phoscorites.

anclyite) are also observed. It also contains various sulfide minerals such as pyrrhotite, pyrite, chalcopyrite and sphalerite.

Pyrochlore is the major rare-metal-bearing mineral in the Sokli PCC. Textural evidence indicates that pyrochlore crystallized relatively later, after crystallization of most other magmatic minerals such as forsterite, magnetite, calcite, phlogopite and baddeleyite. At Sokli, pyrochlore began to crystallize in the stage 2 rocks and continued up to the latest D5 dolomite carbonatite. Baddeleyite, rather than pyrochlore, crystallizes in the first stage P1-C1 rocks, but its crystallization abruptly decreases towards stage 3.

In the P2 phoscorite, pyrochlore occurs as reddish brown octahedra commonly having corroded and embayed yellowish orange outer rims (Fig. 2a) and occasionally overgrows in the marginal part of baddeleyite grains.
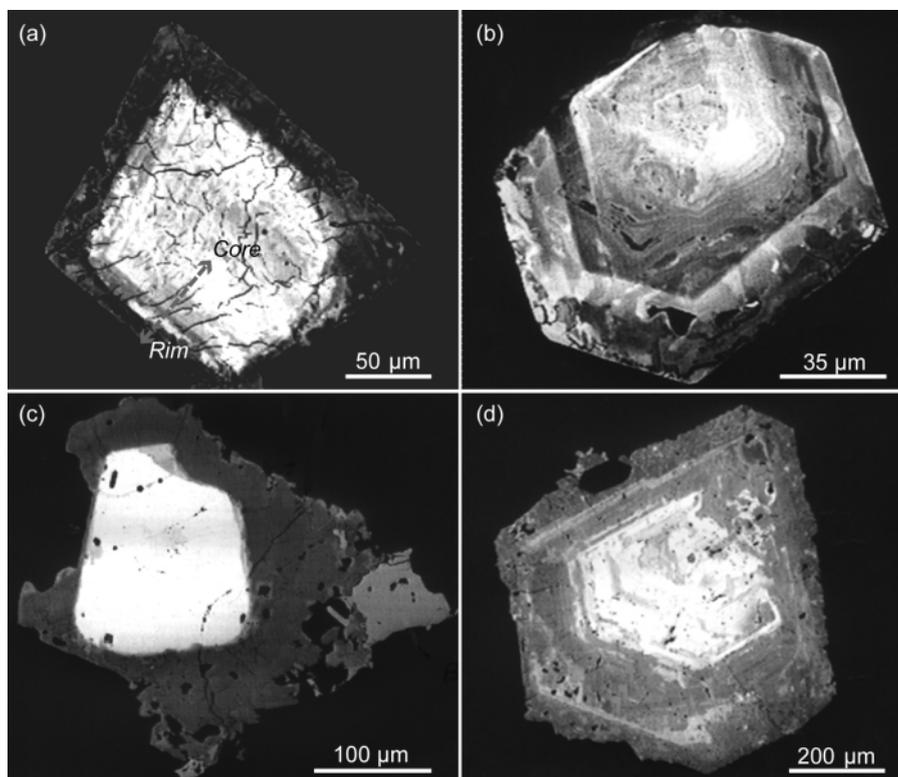
Fig. 3. Backscattered electron images of representative pyrochlore from Sokli. (a) Euhedral C2 pyrochlore with abundant internal fractures and high A-site cation deficiency. The dashed arrow indicates the traverse section of analyses compiled in Fig. 6. Ba-Si-enrichment appears in the bright part (between mid gray and dark gray) of the margin. (b) Euhedral C3 pyrochlore illustrating primary oscillatory zoning and patch alteration in the margin. (C) P2 pyrochlore having euhedral U-Ta-rich (bright) core and Th-rich (dark grey) reserved rim. (d) P3 pyrochlore showing oscillatory magmatic zoning.

Pyrochlore crystals vary in size, but are typically larger than 2 mm. The largest pyrochlore grain reaches up to 5 mm in width. Pyrochlore in the C2 carbonatite occurs as reddish brown euhedral cubes or octahedral, but generally lacks the corroded yellowish orange rims (Fig. 2b). The P3 phoscorite contains the largest amount of pyrochlore. The majority of pyrochlore in the P3 phoscorite is subhedral to anhedral yellowish gray crystals ranging from 2 to 5 mm in size and shows turbid appearances (Fig. 2c). Some pyrochlore grains in the P3 phoscorite are observed within later sulfide veins. Occasionally, small (<0.1 mm) euhedral pyrochlore grains associated with elongated fluorapatite aggregates are observed in the carbonate matrix that fills the interstices between the early crystallized minerals. This late pyrochlore in P3 is usually homogeneous and has almost the same composition with that of the D4 carbonatite. Pyrochlore from the C3 carbonatite is usually fine-grained and euhedral to subhedral (Fig. 2d). In the D4 and D5 carbonatites, pyrochlore is relatively rare and occurs as very small, euhedral to subhedral grain (<0.1 mm).

ANALYTICAL PROCEDURE

Using a Cameca SX 50 at the Natural History Museum, London, more than 600 electron microprobe analyses, including high resolution traverses, were made on pyrochlore in fresh samples from main rock types of the Sokli PCC, except for the P1C1 rocks, in which no pyrochlore found. Analytical conditions of 20 kV accelerating voltage and 25 nA probe current and a PAP $\phi\rho z$ matrix correction procedure were used. Well-characterized natural minerals, pure metals and synthetic compounds including $NaNbO_3$ were used as standards. The results are summarized in Table 1.

CHEMICAL VARIATION OF THE SOKLI PYROCHLORE

Pyrochlore group minerals are characteristic constituents of carbonatites, phoscorites and related metasomatic rocks. These minerals show a wide compositional range with respect to A- and B-site cation substitutions. General formula can be written as $A_{2-m}B_2O_6Y_{1-n}{\cdot}pH_2O$, where
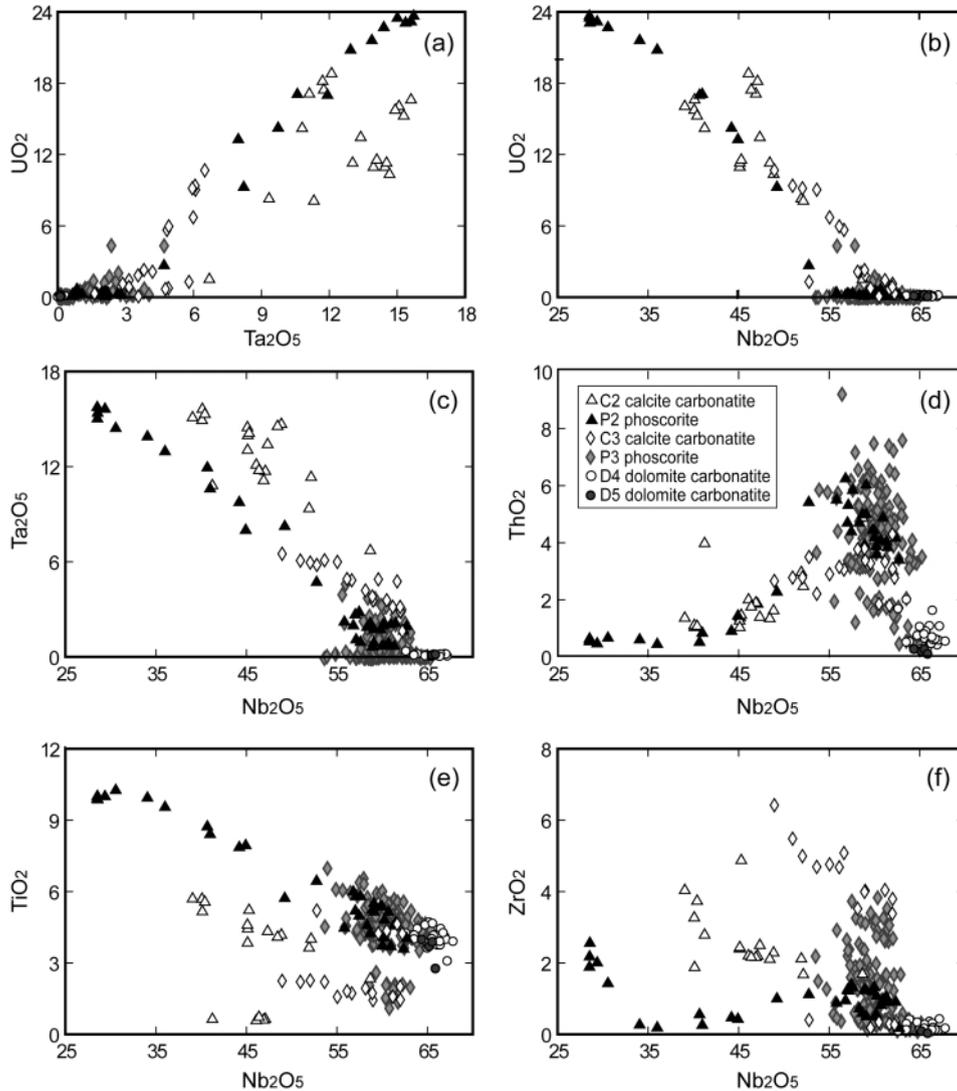
Fig. 4. Compositional variations (in wt.%) of pyrochlore from the Sokli PCC.

A = Na, Mg, K, Ca, Mn, Fe^{2+}, Sr, Sb, Cs, Ba, REEs, Pb, Bi, Th and U; B = Nb, Ta, Ti, Zr, Sn, W, Fe^{2+} and Al; and Y = F, OH, or O (Lumpkin and Mariano, 1996). Structural formulae of the analyzed Sokli pyrochlore have been calculated based on a fixed total of 2.0 *B*-site cations, because large cation vacancies in the *A*-site could be produced by hydrothermal alteration or weathering (Wall *et al.*, 1996; Williams *et al.*, 1997). All pyrochlore grains analyzed in this study belong to the pyrochlore subgroup (Nb + Ta > 2Ti and Nb > Ta, Hogarth, 1977).

Pyrochlore from P2-C2

Pyrochlore in the Sokli PCC generally has complex compositional zoning that can be seen in backscattered electron images (Fig. 3). Early crystallized pyrochlore grains in the P2-C2 rocks are characterized by high U

(up to 24% UO_2, 0.4 a.p.f.u.) and Ta (up to 15.6% Ta_2O_5, 0.33 a.p.f.u.) contents.

Zoned pyrochlore in P2 usually consists of a U-Ta rich, reddish brown euhedral core and a xenomorphic overgrowth of grayish yellow pyrochlore (U-Ta poor and Th rich). Pyrochlore in C2 is usually consists of reddish brown euhedral cubes or octahedra without Th-rich overgrowth in general. The overgrown rim in the C2 pyrochlore is usually thin, slightly resorbed and occasionally enriched in Ba (Fig. 3b).

Figure 4 illustrates the compositional variation of pyrochlore from the Sokli PCC. The variation of UO_2 against Ta_2O_5 shows a strong positive correlation. However, at any given Ta content, the C2 pyrochlore has relatively lower U than that of the P2 pyrochlore. Considering the large *A*-site cation deficiency of the C2 pyrochlore
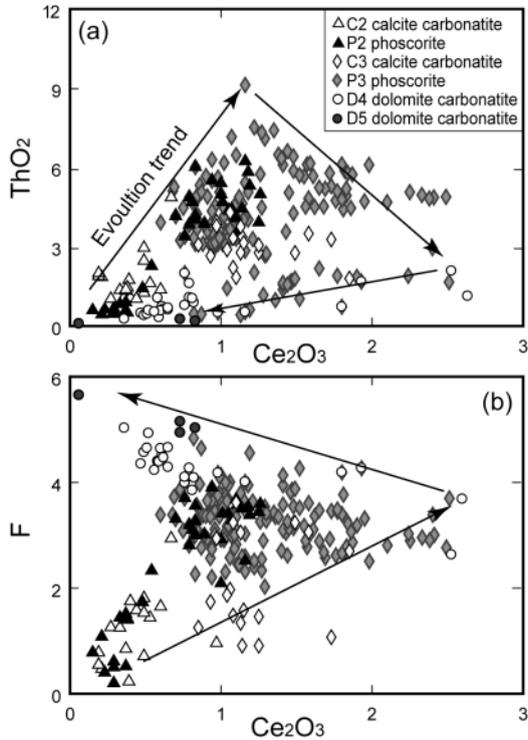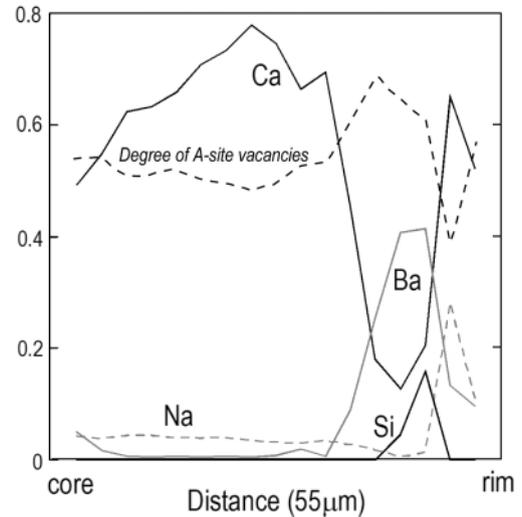
Fig. 6. Compositional profiles (a.p.f.u) of representative C2 pyrochlore shown in Fig. 3a. It can be seen that vacancies in the A-site is largely due to Ca loss.

Fig. 5. Binary plots (in wt.%) of (a) ThO_2 vs. Ce_2O_3 and (b) F vs. Ce_2O_3 for the Sokli pyrochlore.

(Table 1), this relative depletion in U is likely to be a result of U loss during hydrothermal alteration. Recent studies (Lumpkin and Ewing, 1995; Lumpkin and Mariano, 1996) have shown that high valence cations of the A-site, such as Th and U, although generally considered as immobile elements, can be lost during hydrothermal alteration, in relation with a cation exchange at the B-site. On plots of Ta_2O_5, TiO_2 and ZrO_2 against Nb_2O_5, the compositions of the P2 pyrochlore are clearly distinguished from those of the C2 pyrochlore: Ta and Zr are higher in the C2 pyrochlore, whereas Ti is higher in the P2 pyrochlore. These differences seem to be derived from their different mineral parageneses due to differences in their melt compositions. It is noted that overgrowths or marginal parts of the P2 pyrochlore have similar compositions with the P3 pyrochlore (Nb_2O_5-rich P2 pyrochlore in Fig. 4).

Pyrochlore from P3-C3

Among the studied rocks, the P3 phoscorite contains the largest amount of pyrochlore. The majority of the P3 pyrochlore is the Th-Ce-rich type (up to 9.1 wt.% ThO_2 and 2.5 wt.% Ce_2O_3). However, a few grains have transitional compositions between the representative stage 3 pyrochlore and the D4 pyrochlore, i.e., low Th, moderate Ce, and high F contents (Fig. 5). Such compositions are

found in the rims of the typical P3 pyrochlore, or in euhedral discrete grains in the carbonate matrix filling the interstices between early crystallized minerals (magnetite and/or phlogopite).

The C3 pyrochlore shows a more restricted compositional variation compared to the P3. In variation diagrams of UO_2, Ta_2O_5 and ThO_2 against Nb_2O_5 (Fig. 4), the C3 pyrochlore falls in the region between those occupied by the early stage P2-C2 and the P3 pyrochlore, i.e., the C3 pyrochlore has a moderate enrichment in U (about 5 wt.% UO_2) and Ta (about 5 wt.% Ta_2O_5), and a medium level of Th. The plot of TiO_2 versus Nb_2O_5 (Fig. 4e) clearly illustrates that evolution trends of pyrochlore from the phoscorites and carbonatites differ from each other. The trend of the carbonatites is slightly shifted towards lower Ti compared to that of the phoscorites. Another remarkable feature of the C3 pyrochlore is the highest content of Zr among the Sokli pyrochlore varieties (Fig. 4f).

Pyrochlore from D4 and D5

Pyrochlore is relatively rare in the D4 and D5 dolomite carbonatites. Pyrochlore compositions are largely similar in these two dolomite carbonatites. It occurs as subhedral to anhedral grains of very small size (<100 μm). It is chemically homogeneous and close to that of the end-member pyrochlore with the formula $(Ca,Na)_2Nb_2O_6F$) (Table 1). In variation diagrams (Figs. 4 and 5), the D4-D5 pyrochlore always falls at the last extension of the evolution trend of the P3 pyrochlore. They have the lowest contents of U, Ta and Th, and the highest F and Nb contents compared to the other varieties. The variation
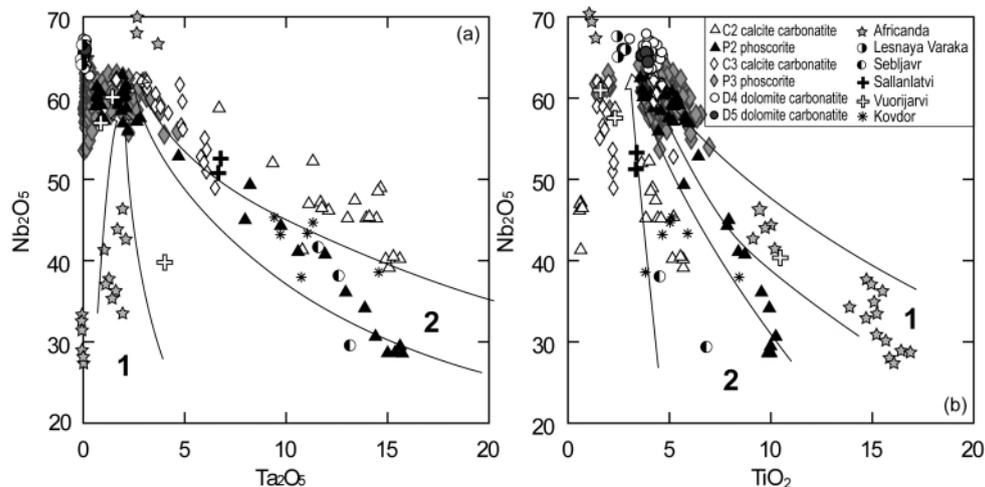
Fig. 7. Compositional variation in pyrochlore-group minerals from the Kola carbonatite occurrences. Two major evolution trends of pyrochlore group minerals in carbonatites and related rocks are illustrated with two broad arrows (1: the betafite and 2: uranpyrochlore). Previous data sources: Vuoriyarvi, Epshtein et al. (1991); Kovdor, Williams (1996); Lesnaya Varaka, Chakhmouradian and Mitchell (1998); Sallanlatvi and Seblyavr, Chakhmouradian and Zaitsev (1999).

of Ce follows a trend similar to that of Th, but the maximum enrichment is reached in the D4 pyrochlore rather than in the P3 pyrochlore in which the highest Th content is found. The Ce content of the majority of the D4 and D5 pyrochlore is comparable to that of the C2 pyrochlore (Fig. 5).

Depletions of Ce and Th in the D4-D5 pyrochlore can be explained by the intensive fractionation of these elements through the crystallization of Ce-Th-rich pyrochlore in the former stage. This is one of the strong links between stage 3 and the late stages.

Alteration trend

Abundant internal fractures and patch alterations are clearly observed in pyrochlore from the C2 and C3 calcite carbonatites (Figs. 2 and 3). This is reflected in the large A-cation deficiency (up to 58% of vacancies in the A-site, Table 1) and low totals of pyrochlore in the calcite carbonatites, which suggests an extensive hydration. Traverse microprobe analyses on an altered grain (from the C2 pyrochlore in Fig. 3a) indicate that the A-site vacancy of pyrochlore in the calcite carbonatites is mainly derived from the loss of Ca and to some extent of Na (Fig. 6). Regions having the A-site cation deficient occasionally show high Ba content (up to 16 wt.% BaO, 0.42 a.p.f.u.), which corresponds to visibly altered parts of the grain. Figure 6 also shows that there is a negative correlation between Ba and Ca contents and a positive correlation between Ba and Si. The elevation of Ba and Si contents with high deficiency of the A-site cations in largely altered parts is also reported from the Bingo and Lueshe pyrochlores (Williams *et al.*, 1997).

Comparison with pyrochlore group minerals from the Kola carbonatites

Wide varieties of pyrochlore group minerals were identified from the Kola carbonatites. The early generations of pyrochlore group minerals are commonly enriched in U, Ta, Th and Ti, whereas, the late generations typically approach the composition of end-member pyrochlore (Chakhmouradian and Williams, 2004). This evolution trend of pyrochlore is also found at the Sokli PCC. The compositions of the Sokli pyrochlore along with those from the other Kola carbonatite complexes are shown in Fig. 7. Two major evolution trends, defined by Chakhmouradian and Zaitsev (1999), are also illustrated. The overall evolution trend of the Sokli pyrochlore is similar to the "uranpyrochlore" trend characterized by the progressive depletion in Ta combined with decreasing Ti. However, when compared with the "uranpyrochlore" trend having the same Nb contents, pyrochlore of the carbonatites is enriched in Ta (Fig. 7a), while that of the phoscorites enriched in Ti (Fig. 7b).

DISCUSSION

Evolution of the Sokli pyrochlore

It was shown in this study that pyrochlore from the phoscorites and associated calcite carbonatites at Sokli systematically change in composition from stage to stage. The early pyrochlore has high contents in U and Ta; these elements suddenly decrease in the intermediate stage pyrochlore, while Th and Ce increase. The late generation is low in Ta, U, Th and Ce, and correspondingly high in Nb (Figs. 4 and 5).

Overall evolutions of Th, Ce and F in pyrochlore from the phoscorites and associated carbonatites can be explained by a unique scheme, but the variations of U, Ti and Zr are rather complex (Figs. 4 and 5). Another remarkable difference is that pyrochlore from the phoscorites always has more evolved margins compared to that of the same stage carbonatites. The relatively lower U content in the C2 pyrochlore compared to the paired P2 pyrochlore is considered to be a secondary aspect as examined in the preceding section. However, the different evolution trends of Ti and Zr and larger compositional ranges of pyrochlore from the phoscorites, compared to that of the paired carbonatites, are certainly primary nature. This provides some critical points for the genesis of the Sokli PCC. First, it is considered that the chemical compositions of the systems during the crystallization of pyrochlore were different from each other. Second, the differences can be interpreted as a result of the different Ti/Nb and Zr/Nb ratios of the melts, or the different mineral paragenesis between phases containing these elements (i.e., magnetite, phlogopite and baddeleyite) in each host rock. The longer and more complex crystallization history of pyrochlore in the phoscorites implies that pyrochlore began to crystallize earlier and continued to later stage under a large temperature interval in the phoscoritic systems. On the other hand, its crystallization in the calcite carbonatites presumably finished during relatively early stage, due to their different melt compositions. Larger A-site vacancy of pyrochlore in the calcite carbonatites compared to that in associated phoscorites is also considered to be resulted from different compositions of their host rocks in which pyrochlore seems to have differently reacted with hydrothermal fluids.

The composition of the D4-D5 pyrochlore is generally homogeneous (no compositional zoning) and distinguished from other varieties. Moreover, they always fall in the last extension of the evolution trend of the P3 pyrochlore in compositional variation diagrams. These characteristics imply that the dolomite carbonatites at Sokli originated from the same phoscorite-carbonatite magma system whose composition had become increasingly dolomitic with differentiation (Wyllie, 1989), rather than from metasomatic processes (Lapin, 1982).

Implications for the genesis of the Kola PCCs

The Kola phoscorites associated with carbonatites have very high Fe, P and Si contents. They are essentially rich in magnetite, apatite and forsterite, and contain subordinate calcite and dolomite. These mineralogical aspects indicate that the parental magma should be enriched in Fe, P and Si and poor in alkali carbonates. Moreover, the intimate field association and strong mineralogical similarity of phoscorites and associated carbonatites from the KAP (Krasnova *et al.*, 2004; Lee *et al.*, 2004; Karchevsky and Moutte, 2004) suggest that these paired rocks originated by differentiation and crystallization from the same Fe-P-Si-rich carbonated parental melts. Recent isotopic results on the Kovdor PCC also support this hypothesis (Zaitsev and Bell, 1995; Amelin and Zaitsev, 2002). It is thus considered that they were derived from a common parental magma and their geochemical contrasts were produced during the separation of these two rocks from a parental magma. However, the segregation processes of the two conjugate rocks are still under discussion. Pyrochlore has not been studied in detail from conjugate phoscorites and carbonatites and so there have been few data available. Therefore, the results of this study, the different chemistry and evolution of pyrochlore from the two paired rocks, provide some new constraints for the relationship and mechanism of segregation between phoscorites and carbonatites.

From a magmatic point of view, we can consider three cases for generating two conjugate rocks, being chemically distinct, but also sharing lots of similarities, from a common parental magma: (1) solid-liquid (magmatic fractionation), (2) solid-solid (coeval accumulation) and (3) liquid-liquid (liquid immiscibility) separations or from a combination of these processes.

We can easily eliminate the first possibility because normal differentiation by accumulation of early crystallizing phases cannot explain the same mineral assemblage and broadly similar mineral compositions between phoscorite and conjugate carbonatite in the same evolutionary stage.

According to the second type of segregation, carbonatites and phoscorites are not fractionated from the other, but coeval crystallization products, more or less cumulative, from the same magma and their distribution in the field results from physical processes (gravity settling, filter pressing and/or elutriation) of segregation operating at the site of emplacement. This type of segregation is well known in normal silicate systems. Particularly, the low viscosity and density of melts and the importance of related fluid activities in carbonatitic systems lead to high sensitivity to segregation process and may help a high degree of sorting between the minerals of a crystal mush. This process would explain the common crystallization history of the two rock types. However, the compositions of the Sokli pyrochlore which crystallized relatively later from the interstitial melts, mostly after the P-C segregation, cannot be simply explained by this hypothesis. In order to explain differences in modal amounts, chemical compositions and evolution trends between pyrochlore in the phoscorites and that in the conjugate carbonatites, it should be assumed that the phoscorites and carbonatites differed in interstitial melt compositions in terms of degree of enrichment for Nb-

Ta-Zr-Hf-U-Th elements and also interelement ratios of these elements. This kind of elemental fractionation is not fully specified in this physical separation process, and thus it requires verification from a chemical viewpoint. Another difficulty in this model is to account for the compositional gap between the two rock types. The expected result of this hypothesis is a layered cumulate having a variable amount of calcite, magnetite and silicates: such a structure is indeed observed in some early carbonatites (C1 and C2), but it does not grade into the phoscoritic composition.

The third one, liquid immiscibility, often appears in discussions on carbonatite genesis as a process to explain the close relationships between alkali silicate rocks and carbonatites (Ferguson and Currie, 1971; Koster Van Groos, 1975; Hamilton *et al.*, 1979; Foley, 1984; Le Bas, 1987, 1989; Kjarsgaard and Hamilton, 1988, 1989; Baker and Wyllie, 1990; Lee and Wyllie, 1996, 1997). Some authors (e.g., Lapin, 1982; Lapin and Vartiainen, 1983) suggested that carbonatitic and phoscoritic materials differentiate from each other by liquid immiscibility. In this case, the two conjugate rocks are products crystallized from two immiscible liquids that were produced by unmixing from a carbonated silicate parental melt enriched in Fe and P. However, this insistence has been mainly based on the petrographical features (i.e., orbicular or spherulitic rocks at Vuoriyarvi and Sokli) rather than chemical evidences because of scant experimental results for liquid immiscibility in the phoscorite-carbonatite system.

Our results, as discussed in the previous section, suggest that different chemical compositions and evolution trends in pyrochlore from two different rock types can better be explained when they have been crystallized from chemically distinctive melts. If liquid immiscibility was responsible for the separation of two rock types, one could test the possibility by comparing the observed chemical compositions with existing experimental data. Unfortunately, there are no experimentally determined partition coefficients for the chemical compositions similar to the studies rocks.

There are a few sets of partition coefficients for carbonate/silicate melt in the literature (Jones *et al.*, 1995; Brooker, 1998; Veksler *et al.*, 1998). The carbonate/silicate melt partition coefficients show the following orders: for major elements, Al < Si < Ti < Fe < Mg < K < Na < Ca < F < P < CO_2, and for trace elements, Hf < Zr < Ta < Tm < Er < Y < Tb < Nb < Sm < Nd < Sr < Ba with some minor inversions between elements of similar behavior. Pressure does not seem to affect the general pattern. In most experiments, partition coefficients increase with increasing degree of immiscibility, however the relative order of preference does not change with the exception of a series of experiments by Brooker (1998).

Relative distributions of some major and trace elements (much higher modal amount of silicates, magnetite and Nb-Zr minerals in the phoscorites) are consistent with the experimental results for carbonate/silicate melts. However, in detail, the geochemistry of the Sokli phoscorites and carbonatites is not always compatible with the experimental data. For example, the ratios of Zr/Nb or K/Al that are expected to be sensitive to liquid immiscibility do not show any significant differences between the Sokli phoscorites and associated carbonatites (Lee, 2002).

The immiscibility that would be relevant in the Sokli PCC is between Fe-Ti-rich and carbonate-rich melts, and it is quite different from that explored in experimental systems between alkali-rich carbonate and silicate melts (Kjarsgaard and Hamilton, 1989; Jones *et al.*, 1995; Brooker, 1998; Veksler *et al.*, 1998). It should be noted that Fe(Ti)-enrichment in phoscorites is even more important than Si-enrichment, hence the relationship between Fe-rich and carbonate-rich systems needs to be explored.

CONCLUSIONS

From the mineralogical and geochemical data for the Sokli pyrochlore obtained in this study, the following conclusions can be drawn.

1. Pyrochlore from the Sokli PCC appears from stage 2; its modal abundance increases strongly up to the percent level in stage 3 and then decreases in stage 4 and 5. It crystallized later than the other major minerals such as forsterite, magnetite, calcite, phlogopite and baddeleyite.

2. The global evolution trend of pyrochlore from the Sokli PCC can be summarized that (i) the early pyrochlore is highly enriched in U and Ta, (ii) in the middle stage, high Th and Ce pyrochlore begins to crystallize and (iii) the late generation in the dolomite carbonatites has composition close to the pyrochlore end member. The Nb/Ta ratio and F content of pyrochlore increase from P2-C2 to the latest D5 dolomite carbonatite.

3. The different compositions and evolution paths of pyrochlore from the two associated rocks imply that the melt compositions from which pyrochlore crystallized were not exactly the same in the two systems, that is, chemical fractionation occurred during the segregation of the two conjugate rocks. Based on the results from this study, together with the previous mineralogical and geochemical studies on the Sokli PCC, we propose a liquid immiscibility process as the most likely segregation mechanism of the phoscorites and associated carbonatites.

4. The unique composition and euhedral morphology of the D4 and D5 pyrochlore as well as a compositional continuity from the early pyrochlore to the latest variety suggest that the dolomite carbonatites are the final mag-

matic products of the Sokli phoscorite-carbonatite system.

REFERENCES

Amelin, Y. and Zaitsev, A. N. (2002) Precise geochronology of phoscorites and carbonatites: The critical role of U-series disequilibrium in age interpretations. *Geochim. Cosmochim. Acta* **66**, 2399–2419.

Barker, D. S. and Wyllie, P. J. (1990) Liquid immiscibility in a nephelinite-carbonatite system at 25 kbars and implications for carbonatite origin. *Nature* **346**, 168–170.

Bell, K., Dunworth, E. A., Bulakh, A. G. and Ivanikov, V. V. (1996) Alkaline rocks of the Turiy Peninsula, Russia, including type-locality turjaite and turjite: a review. *Can. Mineral.* **34**, 265–280.

Brooker, R. A. (1998) The effect of CO_2 saturation on immiscibility between silicate and carbonate liquids: an experimental study. *J. Petrol.* **39**, 1905–1915.

Bulakh, A. G., Ivanikov, V. V. and Orlova, M. P. (2004) Overview of carbonatite-phoscorite complexes of the Kola Alkaline Province in the context of a Scandinavian North Atlantic Alkaline Province. *Phoscorites and Carbonatites from Mantle to Mine: The Key Example of the Kola Alkaline Province* (Wall, F. and Zaitsev, A. N., eds.), 1–43, The Mineralogical Society of Great Britain & Ireland.

Chakhmouradian, A. R. and Mitchell, R. H. (1998) Lueshite, pyrochlore and monazite-(Ce) from apatite-dolomite carbonatite, Lesnaya Varaka comlex, Kola Peninsula, Russia. *Mineral. Mag.* **62**, 769–782.

Chakhmouradian, A. R. and Williams, C. T. (2004) Mineralogy of high-field-strength elements (Ti, Nb, Zr, Ta, Hf) in phoscoritic and carbonatitic rocks of the Kola Peninsula, Russia. *Phoscorites and Carbonatites from Mantle to Mine: The Key Example of the Kola Alkaline Province* (Wall, F. and Zaitsev, A. N., eds.), 293–340, The Mineralogical Society of Great Britain & Ireland.

Chakhmouradian, A. R. and Zaitsev, A. N. (1999) Calcite-amphibole-clinopyroxene rock from the Africanda complex, Kola Peninsula, Russia: mineralogy and a possible link to carbonatites. I. Oxide minerals. *Can. Mineral.* **37**, 177–198.

Dunworth, E. A. and Bell, K. (2001) The Turiy massif, Kola peninsula, Russia: Isotopic and geochemical evidence for multi-source evolution. *J. Petrol.* **42**, 377–405.

Epshtein, E. M., Danil'chenko, N. A. and Nechelyustov, G. N. (1991) Hypogenic bariopyrochlore from a carbonatite complex. *Zap. Vses. Mineral. Obshchest.* **120**, 74–79 (in Russian).

Ferguson, J. and Currie, K. L. (1971) Evidence of liquid immiscibility in alkaline ultrabasic dikes at Callander Bay, Ontario. *J. Petrol.* **12**, 561–585.

Foley, S. F. (1984) Liquid immiscibility and melt segregation in the alkaline lamprophyres from Labrador. *Lithos* **17**, 127–137.

Hamilton, D. L., Freestone, I. G., Dawson, J. B. and Donaldson, C. H. (1979) Origin of carbonatites by liquid immiscibility. *Nature* **279**, 52–54.

Hogarth, D. D. (1977) Classification and nomenclature of the pyrochlore group. *Am. Mineral.* **62**, 403–410.

Jones, J. H., Walker, D., Picket, D. A., Murrel, M. T. and Beate, P. (1995) Experimental investigations of the partitioning of Nb, Mo, Ba, Ce, Pb, Ra, Th, Pa and U between immiscible carbonate and silicate liquid. *Geochim. Cosmochim. Acta* **59**, 1307–1320.

Karchevsky, P. I. and Moutte, J. (2004) The phoscorite-carbonatite complex of Vuoriyarvi, northern Karelia. *Phoscorites and Carbonatites from Mantle to Mine: The Key Example of the Kola Alkaline Province* (Wall, F. and Zaitsev, A. N., eds.), 99–132, The Mineralogical Society of Great Britain & Ireland.

Kjarsgaard, B. A. and Hamilton, D. L. (1988) Liquid immiscibility and the origin of the alkali-poor carbonatite. *Mineral. Mag.* **52**, 43–55.

Kjarsgaard, B. A. and Hamilton, D. L. (1989) The genesis of carbonatites by immiscibility. *Carbonatites, Genesis and Evolution* (Bell, K., ed.), 388–404, Unwin Hyman.

Kogarko, L. N., Kononova, V. A., Orlova, M. P. and Woolley, A. R. (1995) *Alkaline Rocks and Carbonatites of the World: Part 2. Former USSR.* Chapman and Hall, 226 pp.

Koster Van Groos, A. F. (1975) The effect of high CO_2 pressure on alkalic rocks and its bearing on the formation of alkalic ultrabasic rocks and the associated carbonatites. *Am. J. Sci.* **275**, 163–185.

Kramm, U., Kogarko, L. N., Kononova, V. A. and Vartiainen, H. (1993) The Kola Alkaline Province of the CIS and Finland: Precise Rb-Sr ages define 380–360 Ma age range for all magmatism. *Lithos* **30**, 33–44.

Krasnova, N. I. and Kopylova, L. N. (1988) The geological basis for mineral technological mapping at the Kovdor ore deposit. *Int. Geol. Rev.* **30**, 307–319.

Krasnova, N. I., Balaganskaya, E. G. and Garcia, D. (2004) Kovdor—classic phoscorites and carbonatites. *Phoscorites and Carbonatites from Mantle to Mine: The Key Example of the Kola Alkaline Province* (Wall, F. and Zaitsev, A. N., eds.), 99–132, The Mineralogical Society of Great Britain & Ireland.

Lapin, A. V. (1979) Mineral parageneses of apatite ores and carbonatites of the Sebl'yavr massif. *Int. Geol. Rev.* **21**, 1043–1052.

Lapin, A. V. (1982) Carbonatite differentiation process. *Int. Geol. Rev.* **24**, 1079–1089.

Lapin, A. V. and Vartiainen, H. (1983) Orbicular and spherulitic carbonatites from Sokli and Vuorijärvi. *Lithos* **16**, 53–60.

Le Bas, M. J. (1987) Nephelinites and carbonatites. *Alkaline Igneous Rocks* (Fitton, J. G. and Upton, B. G. J., eds.), 53–88, Blackwell.

Le Bas, M. J. (1989) Diversification of carbonatite.

Carbonatites, Genesis and Evolution (Bell, K., ed.), 428–447, Unwin Hyman.

Lee, M. J. (2002) Mineralogy, petrology and geochemistry of the phoscorite-carbonatite association of the Sokli alkaline complex, Finland. Dr. Sci. Thesis, Ecole des Mines de Saint Etienne, 233 pp.

Lee, M. J., Garcia, D., Moutte, J. and Lee, J. I. (2003) Phlogopite and tetraferriphlogopite from phoscorite and carbonatite associations in the Sokli massif, Northern Finland. *Geosci. J.* **7**, 9–20.

Lee, M. J., Garcia, D., Moutte, J., Williams, C. T. and Wall, F. (2004) Carbonatites and phoscorites from the Sokli Complex, Finland. *Phoscorites and Carbonatites from Mantle to Mine: The Key Example of the Kola Alkaline Province* (Wall, F. and Zaitsev, A. N., eds.), 133–162, The Mineralogical Society of Great Britain & Ireland.

Lee, W. J. and Wyllie, P. J. (1996) Liquid immiscibility in the join $NaAlSi_3O_8$-$CaCO_3$ to 2.5 GPa and the origin of calciocarbonatites magmas. *J. Petrol.* **37**, 1125–1152.

Lee, W. J. and Wyllie, P. J. (1997) Liquid immiscibility in the join $NaAlSiO_4$-$NaAlSi_3O_8$-$CaCo_3$ at 1.0 Gpa: implications for crustal carbonatites. *J. Petrol.* **38**, 457–469.

Lee, W. J. and Wyllie, P. J. (1998) Petrogenesis of carbonatite magmas from mantle to crust, constrained by the system CaO-$(MgO+FeO^*)$-(Na_2O+K_2O)-$(SiO_2+Al_2O_3+TiO_2)$-CO_2. *J. Petrol.* **39**, 2005–2013.

Lee, W. J., Huang, W. L. and Wyllie, P. J. (2000) Melts in the mantle modeled in the system CaO-MgO-SiO_2-CO_2 at 2.7 GPa. *Contrib. Mineral. Petrol.* **138**, 199–213.

Lumpkin, G. R. and Ewing, R. C. (1995) Geochemical alteration of pyrochlore group minerals: pyrochlore subgroup. *Am. Mineral.* **80**, 732–743.

Lumpkin, G. R. and Mariano, A. N. (1996) Natural occurrence and stability of pyrochlore in carbonatites, related hydrothermal systems, and weathering environments. *Materials Research Society Symposium Proceedings* **412**, 831–838.

Sweeney, R. J. (1994) Carbonatite melt compositions in the Earth's mantle. *Earth Planet. Sci. Lett.* **128**, 259–270.

Vartiainen, H. (1980) The petrography, mineralogy and petro-chemistry of the Sokli carbonatite massif, northern Finland. *Bulletin of Geological Survey of Finland*, **313**, 126 pp.

Vartiainen, H. and Paarma, H. (1979) Geological characteristics of the Sokli Carbonatite Complex, Finland. *Econ. Geol.* **74**, 1295–1306.

Veksler, I. V., Petibon, C., Jenner, G. A., Dorfman, A. M. and Dingwell, D. B. (1998) Trace element partitioning in immiscible silicate-carbonate liquid systems: an initial experimental study using a centrifuge autoclave. *J. Petrol.* **39**, 2095–2104.

Wall, F. and Zaitsev, A. N. (eds.) (2004) *Phoscorites and Carbonatites from Mantle to Mine: The Key Example of the Kola Alkaline Province*. The Mineralogical Society of Great Britain & Ireland, 498 pp.

Wall, F., Willimas, C. T., Woolley, A. R. and Nasraoui, M. (1996) Pyrochlore from weathered carbonatite at Lueshe, Zäire. *Mineral. Mag.* **60**, 731–750.

Williams, C. T. (1996) The occurrence of niobian zirconolite, pyrochlore and baddeleyite in the Kovdor carbonatite complex, Kola Peninsula, Russia. *Mineral. Mag.* **60**, 639–646.

Williams, C. T., Wall, F., Woolley, A. R. and Phillipo, S. (1997) Compositional variation in pyrochlore from the Bingo carbonatite, Zaïre. *J. Afr. Earth Sci.* **25**, 137–145.

Wolley, A. R. (1989) The spatial and temporal distribution of carbonatites. *Carbonatites, Genesis and Evolution* (Bell, K., ed.), 15–37, Unwin Hyman.

Wyllie, P. J. (1989) Origin of carbonatites: evidence from phase equilibrium studies. *Carbonatites, Genesis and Evolution* (Bell, K., ed.), 500–545, Unwin Hyman.

Wyllie, P. J. and Lee, W. J. (1998) Model system controls on conditions for formation of magnesiocarbonatite and calciocarbonatite magmas from the mantle. *J. Petrol.* **39**, 1185–1893.

Zaitsev, A. and Bell, K. (1995) Sr and Nd isotope data of apatite, calcite and dolomite as indicators of source, and the relationships of phoscorites and carbonatites from the Kovdor massif, Kola Peninsula, Russia. *Contrib. Mineral. Petrol.* **121**, 324–335.